ANL/PHY/CP--89390
CONF-960675--1

# Nuclear Reaction Studies with Radioactive $^{18}$F Beams at ATLAS

K. E. Rehm[a], M. Paul[b], A. D. Roberts[c], C. L. Jiang[a], D. Blumenthal[a], C. N. Davids[a], P. DeCrock[a], S. M. Fischer[a], J. Gehring[a], D. Henderson[a], C. J. Lister[a], J. Nickles[c], J. Nolen[a], R. C. Pardo[a], J. P. Schiffer[a] and R. E. Segel[d]

[a]Argonne National Laboratory, Argonne, IL
[b]Hebrew University, Jerusalem
[c]University of Wisconsin, Madison, WI
[d]Northwestern University, Evanston, IL

The contribution of the $^{18}$F(p,$\gamma$) reaction to the production of $^{19}$Ne which is the crucial isotope for the breakout from the hot CNO cycle into the rp process, has been investigated in experiments with $^{18}$F beams. Measurements of the cross sections for the $^{18}$F(p,$\alpha$)$^{15}$O and the $^{18}$F(p,$\gamma$)$^{19}$Ne reactions indicate that the contribution from the (p,$\gamma$) route to the formation of $^{19}$Ne is small.

## 1. INTRODUCTION

A number of interesting problems in nuclear structure as well as in nuclear astrophysics can best be addressed by the use of radioactive ion beams. Experiments utilizing these radioactive beams, however, require the development of new detection techniques. Since the radioactive isotope of interest has to be produced with a suitable nuclear reaction the beam intensity of the secondary beam is usually lower than that of stable isotopes by several orders of magnitude. Furthermore, since the reaction chosen for the production of the required isotope generates in most cases a wide spectrum of secondary particles, the beams extracted from the ion source of a radioactive beam facility include many elements and isotopes. Although in some cases special chemical properties or a high-resolution mass separator can be used to enhance one species with respect to another, the beam purity in these experiment remains a serious problem. In a series of runs performed at the ATLAS accelerator of Argonne National Laboratory we have developed high-efficiency and high-resolution techniques for these experiments. In our first studies we have investigated $^{18}$F induced reactions which are important to our understanding of the processes occurring in explosive nucleosynthesis. Experiments using other beams, e.g. $^{56}$Ni and $^{17}$F are under way.



The synthesis of heavier elements in explosive nucleosynthesis in a proton-rich environment is believed to proceed through the nuclide $^{19}$Ne which is produced either directly via the $^{15}$O($\alpha$,$\gamma$)$^{19}$Ne reaction or via the $^{14}$O($\alpha$,p)$^{17}$F reaction followed by the sequence $^{17}$F(p,$\gamma$)$^{18}$Ne($\beta^+$) $^{18}$F(p,$\gamma$)$^{19}$Ne [1]. $^{19}$Ne is then the starting point for the rp-process

## DISCLAIMER

where in a series of radiative capture reactions followed by $\beta^+$ decays nuclei up to $^{56}$Ni and beyond are produced [2]. Since $^{18}$F can also interact with protons via the $^{18}$F(p,$\alpha$)$^{15}$O reaction the 'breakout' from the hot CNO cycle via $^{18}$F is controlled by the ratio of the reaction rates R[$^{18}$F(p,$\alpha$)]/R[$^{18}$F(p,$\gamma$)]. In this experiment we have measured the astrophysical reaction rates for the (p,$\alpha$) and the (p,$\gamma$) reactions on $^{18}$F using a radioactive $^{18}$F beam.

## 2. EXPERIMENTAL DETAILS

The experiments were performed at the ATLAS accelerator system of Argonne National Laboratory using a two-accelerator method for generating the $^{18}$F ion beam. The $^{18}$F material ($T_{1/2}$=110 min) was produced at the medical cyclotron of the University of Wisconsin via the $^{18}$O(p,n)$^{18}$F reaction with 11 MeV protons bombarding an enriched [$^{18}$O] water target. After chemical separations the material was flown to Argonne National Laboratory and installed in the negative ion sputter source of the tandem accelerator which is one of the two injectors of the superconducting linear accelerator ATLAS. A more detailed description of the production method can be found in Ref. [3].

The tandem accelerator produced $^{18}$F ions in their $4^+$ state with energies between 11.7-15.1 MeV. For a typical run of 2 hours the average beam current on target was $\sim 5\times10^5$ $^{18}$F/sec. The resulting beam is a mixture of radioactive $^{18}F^{4+}$ and $^{18}O^{4+}$ ions from the production target with the $^{18}$O being 500-2000 times more intense than the $^{18}$F.

Thin stretched polypropylene ($CH_2$) foils ($\sim$ 60-100 $\mu$g/cm$^2$) were used as targets. For the (p,$\alpha$) reactions particle identification was obtained using the gas-filled magnet method which gives clean mass and Z identification even for particles with energies of about 500 keV/nucleon. Details of this technique are given in Ref. [4]. To improve background suppression the $\alpha$ particles from the p($^{18}$F,$^{15}$O)$\alpha$ reaction were detected with a large-area Si detector, mounted at the appropriate scattering angle in kinematic coincidence with the $^{15}$O ions identified in the spectrograph.

The (p,$\gamma$) measurements were performed with the Fragment Mass Analyzer (FMA) [5] which has a high ($\sim$ 30 %) efficiency for radiative capture measurements using inverse kinematics. In the focal plane of the FMA the incoming particles were identified in a position-sensitive parallel-grid avalanche counter according to their m/q ratio. This detector was followed by a large-volume ionization chamber for Z identification. With this arrangement a suppression ratio of $10^{-12}$ for (p,$\gamma$) reaction products relative to the incident beam has been achieved.

Before the actual experiments with $^{18}$F beams the detection efficiencies of the two experimental setups were determined by measuring the excitation functions for the $^{18}$O-induced reactions p($^{18}$O,$^{15}$N)$\alpha$ and p($^{18}$O,$^{19}$F)$\gamma$, respectively. Fig. 1 shows a comparison of the $^{18}$O(p,$\gamma$)$^{19}$F excitation function measured in inverse kinematics using the FMA (solid dots) with the values given in the literature [6](shaded area).

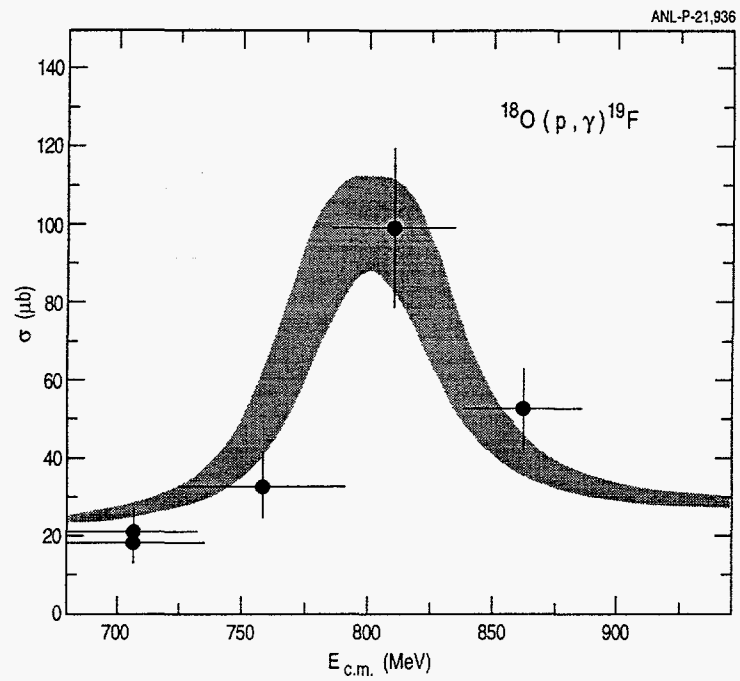


Figure 1. Excitation function for the $^{18}O(p,\gamma)^{19}F$ reaction. The shaded area is calculated with parameters taken from the literature, including a 20 $\mu$b background caused by a small fluorine contamination in the $CH_2$ target.

## 3. EXPERIMENTAL RESULTS

Figure 2 shows the cross sections for the $^{18}F(p,\alpha)^{15}O$ reaction measured in the energy region $E_{cm}$=550-800 keV. The resonance corresponds to a state in $^{19}Ne$ at an excitation energy $E_x$= 7.063 MeV. The horizontal bars represent the energy range due to the energy loss in the $CH_2$ target. The solid line represents a Lorentzian averaged over an energy range of 55 keV which is an average value of the different target thicknesses used in the experiments. From a comparison of the measured proton width $\Gamma_p$ with its Wigner limit and the results of ($^3$He,d) measurements [7] populating states in the mirror nucleus $^{19}F$ a spin value of $3/2^+$ for this state has been derived [8]. This assignment agrees with the results from a thick target measurement for the $^{18}F(p,\alpha)^{15}O$ reaction in Ref. [9]. From a least squares fit to the data values of $\omega\gamma$=2.1±0.7 keV, $\Gamma_p$=5±1.6 keV, $\Gamma_\alpha$=8.6±2.5 keV, and $\Gamma_t$=13.6±4.6 keV were obtained.

For the study of the $^{18}F(p,\gamma)^{19}Ne$ reaction five $^{18}F$ samples were prepared and studied at a bombarding energy of $E_{cm}$= 670 keV, i.e. slightly above the s-wave resonance found in the $^{18}F(p,\alpha)^{15}O$ reaction. The $^{18}F$ beam intensity was monitored by collecting elastically scattered $^{18}F$ particles on a circular aperture covering the angular range $\Theta_{lab}$=3.6°-10° and measuring its $\beta^+$ activity after each run. From the integrated charge associated with the $^{18}F$ beam (2.8 pnC) and the total detection efficiency of the FMA an upper limit for the $^{18}F(p,\gamma)^{19}Ne$ reaction at $E_{cm}$= 670 keV of 42 $\mu$b has been deduced. This value is about a factor of 3 smaller that the one measured in the calibration experiment at the s-wave resonance in the mirror nucleus $^{19}F$ at $E_x$=8.793 MeV.

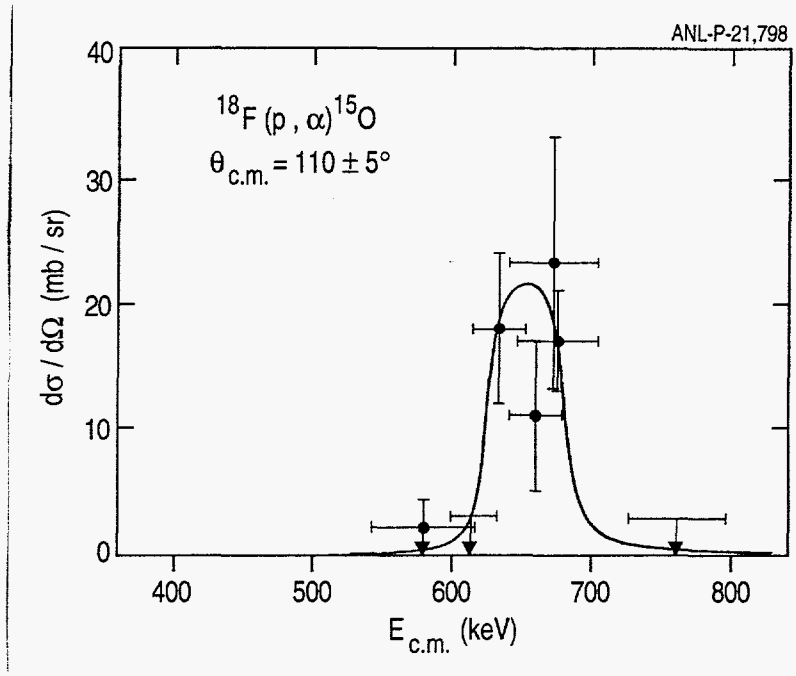


Figure 2. Excitation function for the $^{18}$F(p,$\alpha$)$^{15}$O reaction. The horizontal error bars represent the respective target thicknesses. The solid line represents the cross section from a resonance with parameters given in the text averaged over an energy interval of 55 keV.

Assuming the widths for the $3/2^+$ resonance as given above upper limits for the resonance strength $\omega\gamma$= 740 meV and the gamma width $\Gamma_\gamma$= 3 eV have been calculated. This upper limit for $\Gamma_\gamma$ is comparable to the width obtained for the s-wave resonance populated in the $^{13}$N(p,$\gamma$)$^{14}$O reaction [10] but higher than the upper limit obtained in the system $^{19}$Ne + p [11]. It should be kept in mind, however, that in these experiments considerably higher beam currents were available.

## 4. DISCUSSION

The $3/2^+$ s-wave resonance in $^{19}$Ne has a strong influence on the astrophysical reaction rate for the $^{18}$F(p,$\alpha$) reaction. In order to predict this rate the contributions from other states located in the excitation energy region must be considered. Such calculations are complicated by the fact that not all analog states of $^{19}$F have been located in the mirror nucleus $^{19}$Ne and their resonance strengths are generally not known. Therefore, for lack of any better information on the proton widths, we used the estimate of $\Gamma_p$=0.01*$\Gamma_{sp}$ for negative parity states and $\Gamma_p$=0.1*$\Gamma_{sp}$ for positive parity states in the calculations. The alpha widths $\Gamma_\alpha$ were scaled by penetrabilities from the experimental values of mirror states in $^{19}$F, since by isospin symmetry, the reduced widths for a decay of $^{19}$Ne states to $^{15}$O should be the same as those of $^{19}$F decaying to $^{15}$N [16].

The astrophysical reaction rate is plotted as a function of $T_9$ in Fig. 3 [12]. One can clearly see that the reaction rate above $T_9$=0.5 is dominated by the $3/2^+$ state at 7.063

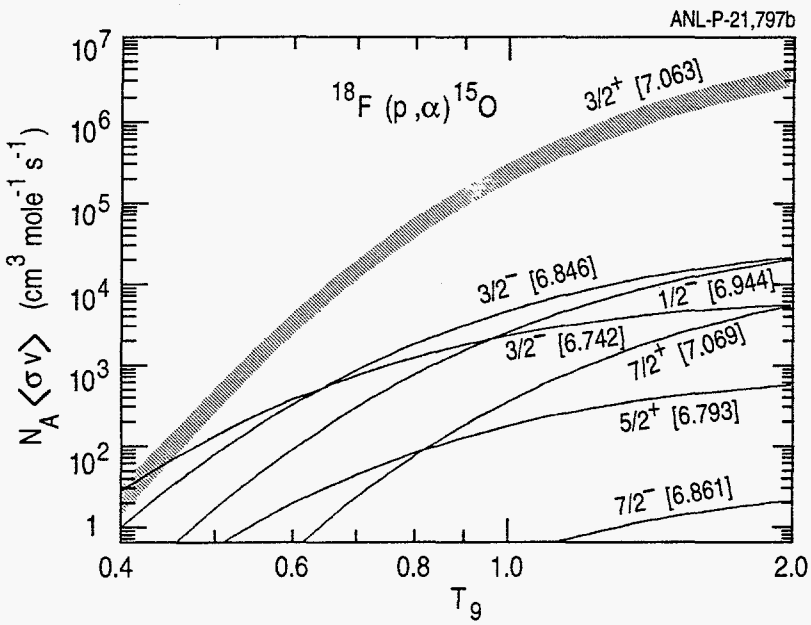


Figure 3. Contributions to the astrophysical reaction rate from several states in $^{19}$Ne[12] as function of the temperature $T_9$.

MeV. Only at temperatures $T_9$ <0.5 do contributions from other states start to be significant with the $3/2^-$ level at 6.742 MeV excitation energy being the most important state.

The controlling factor for the breakout from the hot CNO cycle to the rp-process is the ratio of the reaction rates R[$^{18}$F(p,$\alpha$)]/R[$^{18}$F(p,$\gamma$)]. In the neighbouring nucleus $^{18}$O it was observed that while this ratio is above $10^4$ at temperatures $T_9 > 1$, it drops to about 150 at $T_9 \sim 0.5$ [6]. As a consequence one in about every 150 $^{18}$O + p collisions results in formation of a $^{19}$F nucleus, removing material from the CNO cycle. Our experimental limit for the $^{18}$F(p,$\gamma$) reaction rate together with the prediction from Ref. [15] for the contribution from direct processes restrict the (p,$\alpha$)/(p,$\gamma$) ratio for $^{18}$F to a region limited by the thick and solid lines in Fig.4, respectively. Due to the large value of the $^{18}$F(p,$\alpha$)$^{15}$O cross section the ratio of the reaction rates is above ~1000 for the whole range of temperatures. This means that for the production of $^{19}$Ne the $^{18}$F(p,$\gamma$) route can be neglected and the dominant mechanism for generating this isotope must be the $^{15}$O($\alpha$,$\gamma$) reaction.

## 5. FUTURE DEVELOPMENTS

The two-accelerator method used for the production of $^{18}$F can be applied to other nuclei with suitable half-lifes. Because of the many physics opportunities we have started with the development of a doubly-closed N=Z=28 $^{56}$Ni ($T_{1/2}$=6.1d) beam at the ATLAS accelerator. The $^{56}$Ni source material was produced via the $^{58}$Ni(p,p2n)$^{56}$Ni reaction using a 50 MeV proton beam from the injector to the Intense Pulsed Neutron Source (IPNS) at Argonne National Laboratory. By irradiating an enriched $^{58}$Ni sample and subsequently

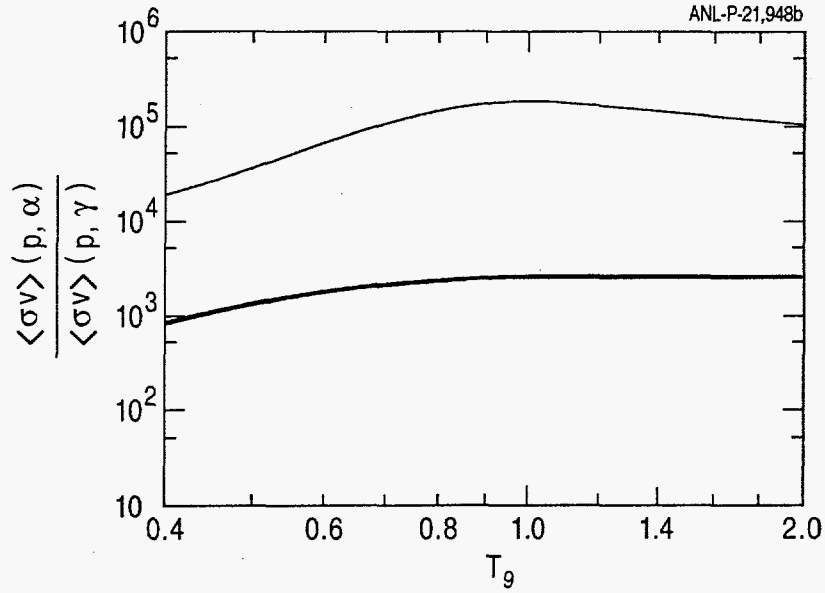


Figure 4. Ratio of the reaction rates between the $^{18}F(p,\alpha)^{15}O$ and the $^{18}F(p,\gamma)^{19}Ne$ reactions. The two solid lines represents the limits to this ratio set by the present experiment.

installing it in the negative ion source of the tandem accelerator at ATLAS, beams of up to 1 ppA of $^{56}Ni^-$ have been extracted from the ion source. Figure 5 shows a particle identification spectrum for 360 MeV mass=56, charge=25 ions, measured at 0° in the focal plane detector of the split-pole spectrograph. In addition to the stable isobar $^{56}Fe$, radioactive $^{56}Co$ and $^{56}Ni$ ions have been observed in this experiment with an intensity ration of 2900 : 8 : 1, respectively. The contribution from $^{56}Fe$ can be reduced by choosing a more suitable pilot beam (e.g. $^{28}Si^{5+}$) for the ATLAS accelerator. Beam currents of several times $10^5$ $^{56}Ni$/sec on target can be expected.

For the production of radioactive beams for isotopes with shorter half-lifes we have utilized the modular structure of the ATLAS accelerator [17]. In a first experiment a $^{17}O$ beam was accelerated in the first section of the accelerator. The inverse $p(^{17}O,^{17}F)n$ reaction in a hydrogen gas target produced $^{17}F$ ions which were transported through the beam line to the experimental station. If the production target is located upstream of the high-energy section of the ATLAS accelerator the last resonators can be used to further accelerate, decelerate or rebunch the $^{17}F$ beam. The first results from bombarding a hydrogen gas target with 71 MeV $^{17}O$ ions are shown in Fig. 6. The particles were again detected at 0° in the focal plane detector of the split-pole spectrograph. The beam contaminant is caused by energy-degraded $^{17}O^{8+,7+}$ ions which have the same magnetic rigidity as $^{17}F^{9+}$. From the results a $^{17}F$ rate at the spectrograph of 400 $^{17}F$/(sec× pnA of $^{17}O$) is calculated. Thus with a production beam current of 250 pnA of $^{17}O$ count rates of $10^5$ $^{17}F$/sec on target can be obtained. Experiments using these two new beams are presently underway.

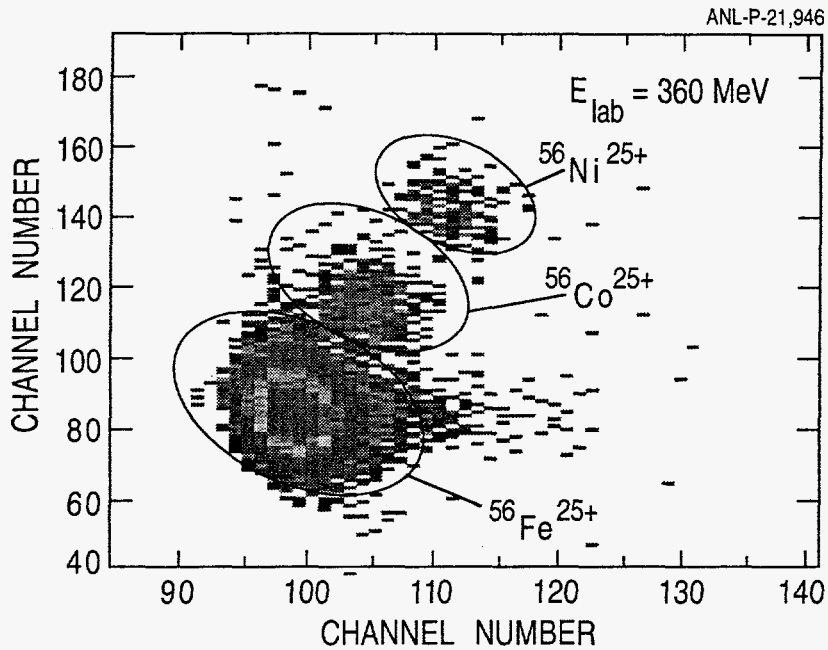


Figure 5. Particle identification spectrum measured for mass $56^{25+}$ ions in the focal plane of the split-pole spectrograph. The various particle groups are due to stable $^{56}$Fe and to radioactive $^{56}$Co and $^{56}$Ni ions produced in the bombardment of $^{58}$Ni with 50 MeV protons.

## 6. SUMMARY

This work provides the first experimental limit for the ratio of the astrophysical reaction rates between the $^{18}$F(p,$\alpha$)$^{15}$O and the $^{18}$F(p,$\gamma$)$^{19}$Ne reactions. The large cross section for the first reaction makes the (p,$\gamma$) route a small branch for the production of $^{19}$Ne which is more effectively produced via the $^{15}$O($\alpha$,$\gamma$) reaction. The gas-filled magnet technique allowed a clean mass and Z identification for reaction products with energies below 1 MeV/u. The use of the Fragment Mass Analyzer for the measurement of radiative capture reactions results is a considerable improvement over gamma detection techniques especially when unstable reaction products have to be detected. Improvements in beam intensity, which should be possible for less chemically reactive unstable isotopes, should allow the use of thinner targets and thus the measurement of excitation functions in finer steps than was done in these first experiments with radioactive ion beams. A program to develop other beams using various production methods is underway.

This work was supported by the U.S. Department of Energy, Nuclear Physics Division, under contract W-31-109-ENG-38 and the National Science Foundation.

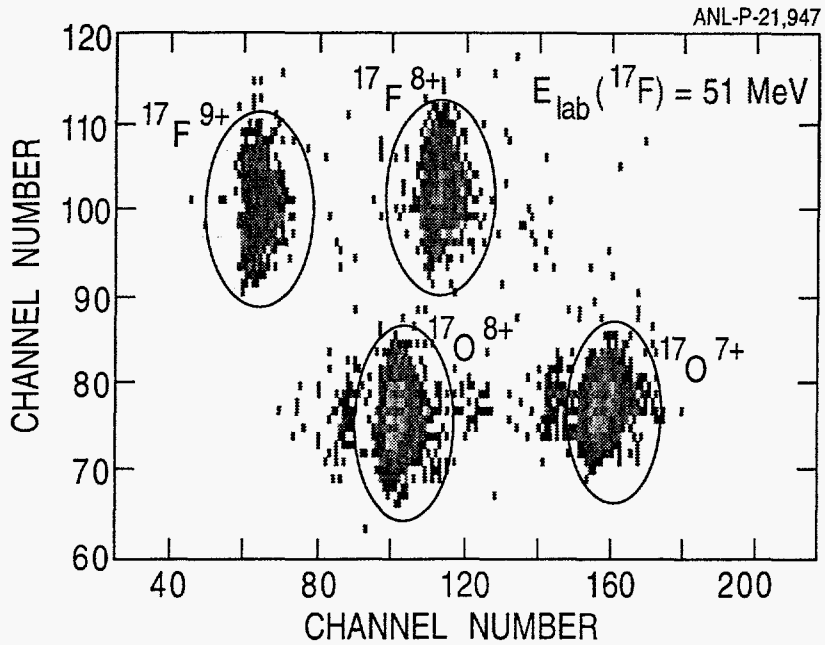


Figure 6. Secondary reaction products identified in the focal plane of the split-pole spectrograph bombarding a hydrogen target with $^{17}$O. The various groups are due to $^{17}F^{9+,8+}$ ions produced via the p($^{17}$O,$^{17}$F)n reaction and energy degraded $^{17}O^{8+,7+}$ ions from the primary beam.

## REFERENCES


1. A. E. Champagne and M. Wiescher, Ann. Rev. Nucl. Part. Sci., **42**, 39 (1992)
2. R. K. Wallace and S. E. Woosley, Astrophys. J. Suppl. **45**, 389 (1981)
3. A. Roberts et al., Nucl. Instrum. Methods **B103**, 523 (1995)
4. K. E. Rehm et al., Nucl. Instrum. Methods **A370**, 438 (1996)
5. C. N. Davids et al., Nucl. Instrum. Methods **B70**, 358 (1992)
6. M. Wiescher et al., Nucl. Phys. **A349**, 165 (1980)
7. C. Schmidt and H. H. Duhm, Nucl. Phys. **A155**, 644 (1970)
8. K. E. Rehm et al., Phys. Rev. **C52**, R460 (1995)
9. R. Coszach et al., Phys. Lett. **B353**, 184(1995)
10. P. Decrock et al., Phys. Rev. Lett. **67**, 808 (1991)
11. R. D. Page et al., Phys. Rev. Lett. **73**, 3066 (1994)
12. K. E. Rehm et al., Phys. Rev. **C53**, 1950 (1996)
13. R. V. Wagoner, Astrophys. Journ. Suppl. **18**, 247 (1969)
14. S. E. Woosley, W. A. Fowler, J. A. Holmes and B. A. Zimmerman, Atom. Data and Nucl. Data Table **22**, 371 (1978)
15. M. Wiescher and K. U. Kettner, Astrophys. Journ. **263**, 891 (1982)
16. F. Ajzenberg-Selove, Nucl. Phys. **A475**, 1 (1987)
17. W. Kutschera et al., Argonne National Laboratory Annual Report ANL-91/12 p.68 (1991), unpublished